A meta-analysis of the inhibin network reveals prognostic value in multiple solid tumors

Eduardo Listik[1†], Ben Horst[1,2†], Alex Seok Choi[1], Nam. Y. Lee[3], Balázs Győrffy[4] and Karthikeyan Mythreye[1]

Affiliations:
[1]Department of Pathology, University of Alabama at Birmingham, Birmingham AL, USA, 35294.
[2]Department of Chemistry and Biochemistry, University of South Carolina, Columbia SC, USA, 29208.
[3] Division of Pharmacology, Chemistry and Biochemistry, College of Medicine, University of Arizona, Tucson, AZ, 85721, USA.
[4] TTK Cancer Biomarker Research Group, Institute of Enzymology, and Semmelweis University Department of Bioinformatics and 2nd Department of Pediatrics, Budapest, Hungary.

Corresponding author:
Karthikeyan Mythreye, Ph.D.
Division of Molecular and Cellular Pathology, Department of Pathology, The University of Alabama at Birmingham.
WTI 320B, 1824 Sixth Avenue South, Birmingham, AL, USA, 35294.
Phone : +1 205.934.2746
E-mail : mythreye@uab.edu

[†]The authors contributed equally to this work.

ABSTRACT

Inhibins and activins are dimeric ligands belonging to the TGFβ superfamily with emergent roles in cancer. Inhibins contain an α-subunit (*INHA*) and a β-subunit (either *INHBA* or *INHBB*), while activins are mainly homodimers of either β_A (*INHBA*) or β_B (*INHBB*) subunits. Inhibins are biomarkers in a subset of cancers and utilize the coreceptors betaglycan (*TGFBR3*) and endoglin (*ENG*) for physiological or pathological outcomes. Given the array of prior reports on inhibin, activin and the coreceptors in cancer, this study aims to provide a comprehensive analysis, assessing their functional prognostic potential in cancer using a bioinformatics approach. We identify cancer cell lines and cancer types most dependent and impacted, which included p53 mutated breast and ovarian cancers and lung adenocarcinomas. Moreover, *INHA* itself was dependent on *TGFBR3* and *ENG* in multiple cancer types. *INHA*, *INHBA*, *TGFBR3,* and *ENG* also predicted patients' response to anthracycline and taxane therapy in luminal A breast cancers. We also obtained a gene signature model that could accurately classify 96.7% of the cases based on outcomes. Lastly, we cross-compared gene correlations revealing *INHA* dependency to *TGFBR3* or *ENG* influencing different pathways themselves. These results suggest that inhibins are particularly important in a subset of cancers depending on the coreceptor *TGFBR3* and *ENG* and are of substantial prognostic value, thereby warranting further investigation.

Keywords: inhibin, activin, endoglin, betaglycan, TGFβ, cancer, prognosis, bioinformatics.

1 INTRODUCTION

Inhibins and activins are dimeric polypeptides members of the TGFβ superfamily, discovered initially as regulators of the follicle-stimulating hormone (FSH).[1-9] Activins are homodimers utilizing different isoforms of the monomeric β_A or β_B subunits located on different chromosomes.[10-12] Inhibin is a heterodimer assembled with an α subunit *(INHA)* and a β subunit (either β_A, *INHBA*, or β_B, *INHBB*). Thus the inhibin naming reflects the β subunit in the heterodimer: inhibin A (α/β_A) and inhibin B (α/β_B), respectively (Fig. 1a).[8,13-16]

Activins, much like TGFβ, signal largely through SMAD2/3.[17,18] Initial receptor binding of activin occurs via type II serine-threonine kinase receptors (ActRII or ActRIIB), which recruit and phosphorylate type I serine-threonine kinase receptors (ActRIB/Alk4 or ActRIC/Alk7) leading to subsequent phosphorylation of SMAD2/3.[8,17,19-22] In multiple tissues, activin signaling is antagonized by inhibin.[23] Thus, the biological and pathological function of activin is directly impacted by the relative levels of the mature α subunit. Inhibins, however, have a much lower affinity for the type II receptors compared to activins themselves which can be greatly enhanced by the presence of the Type III TGFβ receptor, betaglycan *(TGFBR3)*, which binds inhibins' α subunit with high affinity.[8,19,23,24] Thus the most established mechanism of antagonism by inhibin, is via its ability to competitively recruit ActRII preventing activin induced downstream signaling in a betaglycan-dependent manner.[8,19,23,24] This competition model does not allow for direct inhibin signaling. However, conflicting reports on the presence of a separate high affinity inhibin receptor,[25,26] recently discovered interactions of the α subunit with the Type I receptor Alk4,[24] and our recent findings on the requirement of the alternate Type III TGFβ receptor endoglin (*ENG/CD105*) for inhibin responsiveness in endothelial cell function[27] suggest complex roles for inhibins themselves.

Betaglycan and endoglin, are both coreceptors of the TGF-β superfamily with broad structural similarities, [28-30] including glycosylation in the extracellular domain (ECD), a short cytoplasmic domain and common intracellular interacting partners.[31-36] Sequence analysis of betaglycan and endoglin reveals the highest shared homology in the transmembrane (73%) and cytoplasmic domains (61%), with the most substantial difference being in the ECD sequence that impacts ligand binding.[28-30,37-39] Both betaglycan and endoglin knockouts (KOs) are lethal during embryonic development due to heart and liver defects and defective vascular development, respectively, highlighting the shared physiological importance of these coreceptors.[40-43] In contrast to the above described similarities, betaglycan is more widely expressed in epithelial cells, while endoglin is predominantly expressed in proliferating endothelial cells.[44-46]

In cancer, betaglycan and endoglin impact disease progression by regulating cell migration, invasion, proliferation, differentiation, and angiogenesis in multiple cancer models.[34,47-52] Betaglycan acts as a tumor suppressor in many cancer types, as its expression is lost in several primary cancers.[53-55] However, elevated levels of betaglycan have also been reported in colon, triple-negative breast cancers and lymphomas, and has a role in promoting bone metastasis in prostate cancer,[56] indicating contextual roles for betaglycan in tumor progression.[48,57,58] Endoglin is crucial to angiogenesis, and increased endoglin in tumor micro-vessel density is correlated with decreased survival in multiple cancers.[50,59] Evidence in ovarian cancer[60,61] also suggests that endoglin expression may impact metastasis. Inhibins have been robustly implicated in cancer, and

much like other TGF-β members may have dichotomous, context-dependent effects.[62-69] Inhibins are early tumor suppressors, as the *INHA*$^{-/-}$ mice form spontaneous gonadal and granulosa cell tumors.[62] However, elevated levels of inhibins in multiple cancers are widely reported.[63-66,70,71] Active roles for inhibins in promoting late stage tumorigenesis, in part via effects on angiogenesis, have also been demonstrated in both prostate cancer [72] and more recently in ovarian cancer.[27]

Inhibins have been widely used as a diagnostic marker for a subset of cancers[70,71,73] and both betaglycan and endoglin have been evaluated as therapeutic strategies in cancer. TRC-105, a monoclonal antibody against endoglin, was tested in twenty-four clinical trials.[74-97] Current data also suggest benefits of combining anti-endoglin along with checkpoint inhibitors.[98] Similarly a peptide domain of betaglycan called p144 and soluble betaglycan have been tested in multiple cancer types as an anti-TGF-β treatment strategy that decreases tumor growth, angiogenesis, metastasis, and augments immunotherapy.[99-106]

Although prior and emerging studies revealed the dichotomous functions of inhibin's impact on cancer depending on either betaglycan[8,19,23,24] or endoglin,[27] further characterization of the relationship between inhibins-betaglycan-endoglin is vital. This study seeks to provide such prescient information by evaluating the significance, impact, and predictive value of this specific network (*INHA, INHBA, INHBB, TGFBR3,* and *ENG*) by utilizing publicly available genomic and transcriptomic databases.

2 MATERIAL AND METHODS

2.1 Public databases data mining

Clinical data, gene expression alterations, and normalized expression data of RNA-seq were obtained from cBioPortal.[107,108] All available studies were assessed for copy number alterations (CNA) and a subset of cancer for mRNA data (Breast Invasive Carcinoma, Glioblastoma, Lower-grade glioma, Cervical Squamous Cell Carcinoma, Stomach Adenocarcinoma, Head and Neck Squamous Cell Carcinoma, Kidney Renal Clear Cell and Renal Papillary Cell Carcinomas, Liver Hepatocellular Carcinoma, Lung Adenocarcinoma, Ovarian Serous Cystadenocarcinoma, Prostate Adenocarcinoma, Uterine Corpus Endometrial Carcinoma). The results shown here are partly based upon data generated by the TCGA Research Network: https://www.cancer.gov/tcga. Survival data was generated from either KM Plotter[109] or cBioportal (i.e., brain cancers). KM Plotter data for breast, ovarian, lung, and gastric cancer the survival analysis was derived using available gene chip data sets. All others were derived using the RNA-Seq Pan-cancer data sets. The Affymetrix Probe IDs used in gene chip analysis in KM Plotter were: *INHA* (210141_s_at), *INHBA* (204926_at), *INHBB* (205258_at), *TGFBR3* (204731_at), and *ENG* (201808_s_at). Brain cancer data was generated from TCGA Pan Cancer Atlas 2018 dataset for glioblastoma and low-grade glioma. Overall survival (OS) was assessed for all cancer types except ovarian cancer (progression-free survival, PFS) and breast cancer (relapse-free survival, RFS). Gene expression was split into high and low using the median expression. Log-rank statistics were used to calculate the p-value and Hazard ratio (HR).

2.2 Analysis of gene predictiveness to pharmacological treatment

Gene predictive information on treatment regiments was obtained from ROC Plotter (http://www.rocplot.org/).[110] Gene expression for the analyzed genes was compared using the Mann-Whitney U test. Receiver Operating Characteristic (ROC) plots and significance was also computed. ROC curves were compared using Area Under the Curve (AUC) values, and values above 0.6 with a significant p value were considered acceptable.[110] ROC plot assessment was performed in all pre-established categories in ROC Plotter (i.e., breast and ovarian cancers, and glioblastoma). In breast cancer, subtypes (i.e., luminal A, luminal B, triple-negative, $HER2^{+}$) were also analyzed separately. Genes of interest were analyzed for complete pathological response in different pharmacological treatments. All available treatment options were investigated including, taxane, anthracycline, platin and temozolomide. Outliers were set to be removed in this analysis and only genes with a false discovery rate (FDR) below 5% were considered.

2.3 Clustering strategies for genes signatures

From the normalized expression data from RNA-seq studies, the Spearman's ρ coefficient was obtained for *INHA*, *TGFBR3*, and *ENG*. These data were clustered through a Euclidean clustering algorithm using Perseus 1.6.5.0 (MaxQuant). Clusters containing high and low correlations sets were isolated and compared in a pair-wise fashion. The derived genes obtained were checked for protein interaction in BioGRID (thebiogrid.org),[111] and later included in pathway analysis, as described in section 2.5. All plots were performed in GraphPad Prism 8.0.

2.4 Gene signature modeling for prognostics

Gene signature modeling was performed using binary probit regression for each set of cancer types related to *INHA*, *TGFBR3*, *ENG* (Supplementary Table 5), and their respective outcomes (i.e., positive, 1; or negative, 0). The regression was iterated for presenting only significant elements in the following model:

$$\Pr(Y = 1|x_1, \dots, x_k) = \Phi\left(\beta_0 + \sum_{i=1}^{k} \beta_i x_i\right)$$

in which x_i are RNA-seq V2 RSEM expression data for each gene, β_i are obtained coefficients from this regression, Φ is the cumulative normal distribution function. Probability values closer to 1 indicate a positive outcome, while values close to 0, indicate a negative outcome. Postestimation of specificity and sensitivity was also implemented. All regression studies were performed in Stata/SE 16.0.

2.5 Pathway assessment

For pathway analysis, DAVID Bioinformatics Resources 6.8 was used to acquire compiled data from the KEGG Pathway Database.[112] Genes for the analysis were annotated to map to human pathways. The significant outputs were then assessed for the percentage of genes from analyzed

sets and their relevance. To compare pathways between two sets, a pathway significance value ratio ($-\log_{10}R$), in which R is the ratio, was analyzed. Only pathways with an FDR value below 5% were considered.

2.6 Gene dependency Analysis

Gene dependency of *INHA*, *TGFBR3*, *INHBA*, *INHBB,* and *ENG* was analyzed using the DepMap portal (www.depmap.org).[113] Gene expression through Expression Public20Q1 dataset was analyzed via comparing it with RNAi and CRISPR datasets. Perturbed genes with similar trend correlation values with two or more perturbation methods were compiled. Genes commonly affected by perturbation methods were plotted onto a Venn diagram.

3 RESULTS

3.1 Inhibins and activins are altered in human cancer

We and others reported previously diverse roles for members of the inhibin/activin family in cancer.[8,27,114-117] Our and prior mechanistic studies in cancer indicate a strong dependency of inhibin function on betaglycan and endoglin.[24,27,118-121] To begin to evaluate the impact of this relationship more broadly in cancers we analyzed gene alterations including mutations, amplifications, and deletions for the genes encoding inhibin/activin subunits *INHA*, *INHBA*, *INHBB*, and the key coreceptors — *TGFBR3,* and *ENG* (Fig.1a) in all public datasets available in cBioPortal (Fig.1b, Supplementary Table 1). Percentage of patients from the whole cohort that possessed any of the alterations either by themselves or concomitantly was analyzed. We find that melanoma (16.26%), endometrial (13.16%), esophagogastric (10.85%), and lung (10.69%) cancers revealed the highest alterations for the genes. The alterations for the genes varied, with *INHBA* and *TGFBR3* exhibiting higher rates of alterations (0–5.65% and 0.17–3.91% respectively) that also varied by cancer type. The range for *INHA*, *INHBB,* and *ENG* was found to be between 0–2.38%, 0–2.62%, and 0–3.23% respectively (Fig. 1b).

In comparing expression levels of each of the genes in the same TCGA datasets as in Fig. 1b, we find that overall *ENG* is the most highly expressed gene (Fig. 1c) with variance among different cancer types (e.g., lower-grade glioma and cervical *vs.* renal clear cell and lung adenocarcinoma, $p < 0.0001$) and subtypes (e.g., luminal A *vs.* luminal B breast cancers, $p < 0.0001$). Interestingly, *TGFBR3* expression differed most notably between glioblastoma and lower-grade gliomas ($p < 0.0001$), and breast cancers exhibited higher expression as compared to ovarian and endometrial ($p < 0.0001$). *INHBB* in contrast was mostly expressed in renal clear cell and hepatocellular carcinomas, which differs from renal papillary cell carcinoma and cervical cancer ($p < 0.0001$). Both *INHBA* and *INHA* were the least expressed as compared to the others (Fig. 1c). Exceptions were head and neck and esophagogastric cancers that had high expression of *INHBA* and lung adenocarcinoma and renal clear cell carcinoma that had high expression of *INHA*.

While the above analysis examined patient tumors, we next examined cell lines as a way to delineate model systems for future studies. For these analyses, we used the DepMap project

(www.depmap.org)[113] which is a comprehensive library of human genes that have been either knocked down or knocked out through CRISPR technology in 1,776 human cell lines representing multiple cancer types.[122-124] Dependency scores representing the probability of queried gene dependency for each cell line and thereby cancer type is obtained.[125] Here, we find that the ligand encoding gene *INHA* displayed higher dependency than the activin subunit isoforms *INHBA* or *INHBB* or either receptors *TGFBR3* and *ENG* (Fig. 1d). Notably, esophageal, gastric, and ovarian cancers had the highest dependency results for *INHA* (≥ 14%) consistent with the alterations seen in Fig. 1c. Within these cancers, *INHBA* exhibited higher dependency values in ovarian cancer (6%) albeit not as high as *INHA*. Besides *INHBB* in myeloma (6%), no other notable dependency relationships was observed.

In an attempt to identify genes most impacted by alteration to each of the individual genes, we examined how RNAi and CRISPR interventions would affect their correlation to specific genes. Those similarly affected by these techniques were found to be dependent on the investigated set of genes. We find that *ENG* exhibited the highest number of dependent genes (Fig. 1e, n = 71) followed by *INHBA* (57), *INHBB* (49), *TGFBR3* (44) and *INHA* (30) (Fig. 1e, Supplementary Table 1). Interestingly, only a total of 5 genes were commonly dependent between *INHA* and the other genes (Fig. 1e, *MAX* with *INHBA* and *GRPEL1*, *SF3B4*, *ESR1,* and *TFAP2C* with *INHBB).* *INHBA* on the other hand had several common dependent genes most notably 13 genes were common with *ENG* dependency (e.g., *VCL*, *TLN1*, and *LYPD3*).

3.2 Effect of inhibins and the coreceptors on patient survival varies by cancer type

Since alterations in expression of inhibin, activin, *TGFBR3* and *ENG* exist in human cancers and prior studies have implicated each of these in patient outcomes;[27,52,59,71,114,126-129] we conducted a comprehensive analysis of each of these genes on overall survival (OS), progression-free survival (PFS), or relapse free survival (RFS) in a broad panel of cancers. The goal here was to identify the patients and cancer types most impacted by changes in gene expression. Analysis was conducted using datasets in KM Plotter[109](Fig. 2, 3 and summarized in Supplementary Table 2). We find that not all cancers are equally impacted. Of note, we find that in both breast and ovarian cancers all five genes were either positive predictors of survival or non-predictive except *INHBB* in breast (HR = 1.06, p = 0.034) and *INHBA* in ovarian (HR = 1.16, p = 0.047) (Fig. 2). However, in p53 mutated cancers, *INHA* was a strong negative predictor of survival for both breast and ovarian cancers (HR=1.99, p = 0.0056 and HR = 1.55, p = 0.0039, respectively), along with *ENG* in ovarian cancer (HR = 1.36, p = 0.0098, Fig. 2, 3). Additionally, in lung cancers, *INHA* and *ENG* differed from *TGFBR3,* as *INHA* (HR=1.26, p = 0.00029) and *ENG* (HR = 1.20, p = 0.0056) were both negative predictors of survival while *TGFBR3* (HR = 0.65, p = 3.4E-7) was a strong positive predictor of survival (Fig. 2). Specifically, we find that *INHA* and *ENG* are robust predictors of poor survival in lung adenocarcinomas but not in squamous cell carcinomas (Fig. 2, 3). Gastric cancers represent another robust cancer type where all five genes were negatively correlated with survival (Fig. 2, 3). Since *HER2* expression is a frequent abnormality in gastric cancer,[130] we examined if there were any differences in survival associated with *HER2* expression. All five genes in both $HER2^{+}$ and $HER2^{-}$ gastric cancers, except *INHBA* in $HER2^{-}$ gastric cancers, were negatively correlated with survival (Fig. 2). In kidney cancers, *INHA* was a negative predictor of survival in both renal clear cell and renal papillary cell carcinoma (Fig. 2, 3), consistent with

prior findings.[27] *TGFBR3* was a strong positive predictor of survival in both renal clear cell carcinoma (HR = 0.46, p = 2.1E-7) and renal papillary cell carcinoma (HR = 0.53, p = 0.042, Fig. 2, 3). *ENG* (HR = 0.51, p = 8.6E-6) was a positive predictor of survival in renal clear cell carcinoma but not significantly associated with survival in renal papillary cell carcinoma (Fig. 2). Finally, in brain cancers, *INHA* was a negative predictor of survival in glioblastoma but a positive predictor in low-grade gliomas (Fig. 2). Of note, *ENG* appeared to have a lower range of HR values compared to *INHA* and *TGFBR3*. *INHBA* and *INBBB* were not as significantly correlated with survival as *INHA*, *ENG*, and *TGFBR3*. *INHBA* was significantly correlated with 8 cancer types while *INHBB* was significantly correlated with 9. *INHBA* and *INHBB* showed similar correlations with survival in gastric cancers, specifically *HER2*$^{+}$, and renal papillary cell carcinoma (Fig. 2). *INHBA* and *INHBB* showed opposing effects however in liver cancer where *INHBA* (HR = 0.62, p = 0.0086) was a strong positive predictor but *INHBB* (HR = 1.52, p = 0.025) was a potent negative predictor (Fig. 2).

Since inhibin's biological functions have been shown to be dependent on the coreceptors *TGFBR3* and *ENG*, [24,27,118-121] we examined the impact of *INHA* based on the expression levels of each of the co-receptor (Table 1). In this analysis, we find that that when separating patients into high or low expressing *TGFBR3* or *ENG* groups (Table 2) in p53 mutated breast cancers, where *INHA* is a negative predictor of survival in all patients (Fig. 2), *INHA* was only a predictor of poor survival in patients with low *TGFBR3* (HR = 2.29, p = 0.015) or low *ENG* (HR = 2.24, p = 0.035). Interestingly, this trend was also repeated in renal clear cell carcinoma, where *INHA* was only a predictor of survival in *TGFBR3* low (HR = 2.75, p = 9.0E-06) and *ENG* low (HR = 2.6, p = 2.5E-06, Table 1). In contrast to breast and renal clear cell cancers where *TGFBR3* and *ENG* both impacted the effect of *INHA* on survival, *TGFBR3* levels did not change *INHA*'s impact on p53 mutated serous ovarian cancers (Table 1). In *ENG* high p53 mutated serous ovarian cancer patients, *INHA* had a more significant negative prediction outcome (HR = 2.12, p = 1.8E-6) compared to *ENG* low (HR = 0.8, p = 0.18, Table 1). Similar outcomes were observed in lung adenocarcinomas with respect to *TGFBR3,* where *INHA* remained a strong negative predictor of survival in patients regardless of *TGFBR3* expression levels (Table 1). However, *INHA* remained a robust negative predictor of survival in lung adenocarcinomas patients expressing low *ENG* (HR = 2.12, p = 0.00041) but was not significant in *ENG* high expressing patients (HR = 1.25, p = 0.14) (Table 1).

Together, these findings suggest that *INHA* expression as a predictive tool for survival is influenced by the coreceptors *ENG* and *TGFBR3* in renal clear cell, lung, and p53 mutated breast and ovarian cancers. *INHA* is dependent on these coreceptors in all breast and ovarian cancers.

3.3 Inhibins and activins can predict response to chemotherapy in luminal A breast cancer

We next evaluated the pathological response based classification for each of the genes using the receiver operating characteristic (ROC) plotter (www.rocplot.org) to validate and rank *INHA, INHBA/B*, *TGFBR3* and *ENG* as predictive biomarker candidates.[110] In a ROC analysis, an area under the curve (AUC) value of 1 is a perfect biomarker and an AUC of 0.5 corresponds to no correlation at all. We first entered all genes to allow for FDR calculation for each gene at FDR cutoff of 5% (Supplementary Table 3). We next examined individual genes and find that in luminal A breast cancers *ENG*, *TGFBR3*, *INHA,* and *INHBA*, were better performing as compared to

INHBB particularly for taxane or anthracycline based chemotherapy regimens. ROC plots for the two regimens are displayed in Fig. 4 and Supplementary Table 3.

Both *ENG* and *TGFBR3* were predictive in other cancer types as well (Supplementary Table 3). Specifically, while *ENG* performed better in taxane treatments in *HER2*$^{+}$ breast cancer subtype, *TGFBR3* performed better for taxane regimens in triple-negative breast cancer (TNBC) and serous ovarian cancer. Interestingly, examining expression (Fig. 4b) revealed that in the same luminal A breast cancers *INHA, ENG* and *INHBA* are less expressed in responders to pharmacological treatment while *TGFBR3* is more expressed in these responder groups (Fig. 4b). Similar trends for *TGFBFR3* expression were seen in TNBC and serous ovarian cancer groups where *TGFBR3* was more expressed in the responders' group for taxane regimens. *ENG* was also more expressed in *HER2*$^{+}$ breast cancer patients who respond to taxane therapy, which was opposite to the luminal A subtype expression levels (Fig. 4b). Full data for the ROC curve assessment is available in Supplementary Table 3. In summary *INHA*, *INHBA*, *TGFBR3,* and *ENG* display clear discrepant profiles of expression among responders and non-responders to both anthracycline and taxane chemotherapy for distinct breast cancer subtypes, specifically luminal A, and serous ovarian cancer. These genes also harbor a possible predictive value to indicate responsiveness to these therapy regimens. Moreover, *ENG* expression could also differentiate luminal A and *HER2*$^{+}$ breast cancers response to taxane therapy. *INHBB* on the other hand had no predictive value in the assessed cancer types.

3.4 Gene signatures from inhibins can predict patient survival outcomes

Given that *INHA*, *TGFBR3,* and *ENG* impact patient outcomes more broadly and more significantly that *INHBB* and *INHBA*, and the prior direct functional dependency of *TGFBR3* and *ENG* to inhibin function rather than activin[38,131] we examined signatures associated with either a negative or positive outcome for each of the three genes. Cancer types that presented different survival predictions for *INHA*, *TGFBR3,* or *ENG* were assessed (Fig. 5a), and cancer types in which each gene would have a similar patient outcome (i.e., positive overall survival outcome *vs.* negative overall survival outcome) were separated into groups (e.g., *INHA* positive outcome *vs*. negative outcome, Fig. 5a).

Spearman's ρ coefficient was calculated for all RNA-seq gene data provided in each of these datasets, and values were clustered, and genes that were either positively and negatively correlated with each individual *INHA, TGFBR3* or *ENG* genes were identified (Supplementary Table 4). The top correlated genes from the positive outcome set were then pairwise compared to genes that had lower correlations in the negative outcome set, and vice-versa to obtain a subset of common genes.[132-135] Examples include *TGFB2* and *HOXA1* where genes correlated to *INHA* in the negative outcome set, and *OGG1* and *STAP2* in the positive outcome group. For *TGFBR3*, *AP1M1* and *RILPL1* correlated in the negative outcome context, while *FZD5* and *MYCN* in the positive one. No gene signatures were obtained for *ENG*. As indicated in section 3.2, the HR value range was the smallest for *ENG* in the assessed cancer types, which limits the differential gene signature analysis. All these genes also had their mRNA expression assessed in the respective cancer sets, contrasted, and evaluated for difference in expression (Fig. 5b). Except for 22 genes

from sets in which *INHA* or *TGFBR3* had distinct predictions of survival (e.g., *CHSY1, LDLR*, *PPARG*, *MIA2*, *TOX3*) all others exhibited significant alterations in gene expression (Fig. 5b).

The altered genes from Fig. 5b whose difference in expression was significant, were assessed for protein interactions and these iterated for pathway analysis using BioGRID (thebiogrid.org, Fig. 5c).[111] We find that *INHA* gene sets were associated with either *PD-L1* expression and PD-1 checkpoint, Rap1 signaling pathways in patients with positive outcomes or cell cycle regulation in patients with negative outcomes. *TGFBR3* associated genes on the other hand, relied on *VEGF* and *MAPK* signaling pathways for patients with positive outcome and *IL-17*, *p53*, or even *Wnt* signaling pathways in the negative outcome scenario. Detailed descriptions of analyzed genes and pathways are compiled in Supplementary Table 4.

To determine if the genes associated with *INHA* and *TGFBR3* had true prognostic value, a Probit regression model was applied to the normalized mRNA expression of the genes in Supplementary Table 5. The regressions were analyzed for the cancers from Fig. 2a and Fig. 2d which had clear outcomes for either *INHA*, or *TGBFR3*. The final coefficients and entry genes are also provided in Supplementary Table 5. We find that the *INHA* model had 43 genes as dependent elements, and the *TGFBR3* model had 37 genes. However, the most suitable model obtained from these sets is the *TGFBR3* model, which has a high goodness of fit p-value ($p = 0.9494$), sensitivity (98.42%), specificity (91.56%), and accuracy (96.70%, Table 2).

These analyses reveal that a differential signature obtained from *INHA*, along with one of its main binding receptors (i.e., *TGBFR3*) are able to faithfully predict a patient's outcomes in a wide spectrum of cancer types (e.g., kidney, lung, head and neck, breast, liver, ovarian, stomach, endometrial).

3.5. Functional analysis and interpretation of inhibin's mechanism of action

Prior functional studies indicate a dependency on *ENG* and *TGFBR3* for inhibin responsiveness.[38,131] To test if these biological observations hold in patient datasets, we performed supervised clustering using Euclidean algorithm of genes correlating with either *INHA, ENG* or *TGFBR3* using the RNA-seq data for cancer types with the most significant impact as determined in Fig. 6a. Only the most enriched transcripts that were either positively or negatively correlated transcripts are shown in Fig. 6a. Most enriched genes from these clusters were then compared amongst each other in all pairwise combinations for similarities (e.g., positively correlated to *INHA vs.* negatively correlated to *TGFBR3*, and so on, Fig. 6b).

We find that *INHA* and *TGFBR3* comparison rendered 1,430 genes, in which 24.6% were exclusive to *INHA* (e.g., *DLL3*, *GPC2*, *TAZ*, *TERT*, *XYLT2*) 37.7% to TGFBR3 (e.g., *CCL2*, *CCR4*, *EGFR*, *GLCE*, *IL10RA*, *IL7R*, *ITGA1*, *ITGA2*, *JAK1*, *JAK2*, *SRGN*, *SULF1*, *TGFBR2*), and 13.1% were positively correlated to both (e.g., *CSPG4*, *COL4A3*, *FGF18*, *NOTCH4*, *SMAD9*). When *INHA* was assessed with respect to *ENG* we find 1,773 genes of which, 11.2% were exclusive to *INHA* (e.g., *GDF9*, *PVT1*), 21.3% to *ENG* (e.g., *CCL2*, *GPC6*, *IL10*, *IL10RA*, *IL7R*, *INHBA*, *ITGA1*, *ITGB2*, *JAK1*, *SRGN*, *SULF1*, *TGFB1*, *TGFBR2*) and 10.0% were highly correlated to both (e.g., *CSPG4*, *DLL1*, *FGF18*, *FZD2*, *NOTCH4*). Lastly, the comparison between *ENG* and

TGFBR3 returned 1,938 genes. However, very few were exclusive to either *TGFBR3* (2.84%) or *ENG* (0.16%), revealing a high functional resemblance between both of these receptors, as most of the profiled genes correlated to both of them (48.5%, e.g., *ADAM9*, *-23*, *ADAMTS1*, *-2*, *-5*, *-8*, *-9*, *CCL2*, *CSF1R*, *DLL4*, *ESR1*, *FGF1*, *FGF2*, *FGF18*, *GLI1*, *-2*, *-3*, *GPC6*, *IL10RA*, *ITGA1*, *ITGA5*, *JAK1*, *MMP2*, *SDC3*, *SRGN*, *SULF1*, *TGFB3*, *TGFBR2*, *TNC*, *TWIST2*, *XYLT1*, *ZEB1*) or none of them.

We next used each gene set from the cross-comparisons in Fig. 6b to identify pathways using KEGG.[136] Unique pathways with an FDR below 5% were identified for the comparisons and are presented in Fig. 6c. Although several common pathways were present between groups, such as PI3K-Akt and Ras signaling pathways (see Supplementary Table 6), some unique pathways were present as well. *ENG*, for instance, was more exclusively related to cytokine-cytokine receptor interaction and natural killer mediated cytotoxicity (Fig. 6c), while *TGFBR3* was more exclusively related to proteoglycans interaction and chemokine signaling. While cell cycle and DNA replication were not directly associated with *ENG* and *TGFBR3*, Rap1 signaling and Extracellular matrix (ECM)-receptor interactions were both impacted by *ENG* and *TGFBR3* (Fig. 6c). However, no independent pathway could be pinpointed to *INHA* alone, revealing dependency on either *TGFBR3* or *ENG*. These studies indicate that inhibin's effects may vary depending on whether *ENG* is more highly expressed as compared to *TGFBR3* with significant relevance to defining mechanism and impact of changes in components of this pathway.

4. DISCUSSION

This study aimed to evaluate comprehensively the influence of the inhibin-activin network in cancer. Our findings provide significant new information on the specific cancers impacted by the genes investigated here, *INHA, INHBA, INHBB, ENG* and *TGFFBR3*, and shed light on potential functional dependencies. Additional gene signature analysis reveals that *INHA*, along with one of its main receptors (i.e., *TGBFR3*) faithfully predicts patient outcomes in a wide spectrum of cancer types.

TGFβ1 is a representative member of the TGFβ family that has been significantly investigated previously.[137] However, less information exists about the precise impact and role of other members like inhibins and activins. Our findings that *INHA* is significantly associated with survival in sixteen of the twenty-one cancers analyzed, correlating positively with survival in six cancers and negatively in ten (Fig. 2), highlight *INHA*'s differential role as a tumor suppressor or promoter depending on the specific cancer type. In highly angiogenic tumors like renal clear cell carcinoma[138] and glioblastoma,[139] we found *INHA* expression to be a significant negative predictor of survival. *INHA*'s role in promoting tumorigenesis in these cancer types may occur through its effects on angiogenesis as has been previously reported for a subset of ovarian and prostate cancer[27, 72] warranting further investigation. In Luminal A breast cancers, we observed that increased *INHA* expression was associated with unresponsiveness to chemotherapy (Fig. 4) while in survival data it was a positive predictor of survival (Fig. 2). This apparent contradiction can perhaps be explained by the fact that data in KM Plotter contains information on patients that have undergone a wide array of treatments. Likely, *INHA* is predictive of response to some treatments but not others. Curiously, in both breast and ovarian cancers, *INHA* was only a negative predictor

of survival in patients that had p53 mutations indicating a potential dependency of *INHA* functions on the p53 status. *INHA* expression alterations have been observed in p53 mutated adrenocortical tumors and *INHA* was suggested to be a contributing factor to tumorigenesis in these cancers.[140] One of the most characterized transcriptional activators of *INHA* is GATA4,[141] which can also regulate p53 in cancer and could be responsible for the different survival outcomes we see for *INHA* in p53 mutated cancers versus wild-type p53 cancers.[142,143] *INHA* expression changes and the link to functional outcomes in the background on p53 mutations remains to be fully elucidated.

Between the TGF-β family co-receptors (*ENG* and *TGFBR3)* implicated in cancer progression and inhibin function, *ENG* was more expressed (Fig. 1c), particularly in lung adenocarcinoma and gastric cancers, corresponding with *ENG* being a strong negative predictor of survival (Fig. 1c, 2). These findings are consistent with prior experimental findings as well.[144,145] In p53 mutated cancers, *ENG* remained a negative predictor. ROC Plotter analysis revealed decreased *ENG* expression to be associated with response to anthracycline therapy in Luminal A breast cancer patients (Fig. 4). However, a previous study showed that positive *ENG* expression was associated with increased survival in breast cancer patients who had undergone anthracycline treatment.[146] While Isacke and colleagues did not report a specific subtype in their analyzed cohort,[146] we obtained significant results for Luminal A breast cancer, specifically. Moreover, an additional study performed in acute myeloid leukemia showed an inverse relationship to that of Isacke et al., consistent with our results in Luminal A breast cancer.[146,147] We also found *ENG* to be a predictive of response to taxane therapy regimens. An inverse relationship between *ENG* expression was observed in responders for Luminal A and *HER2*$^+$ breast cancer, with responders expressing high *ENG* in *HER2*$^+$ breast cancers but low levels of *ENG* in Luminal A cancers (Fig. 4). As Luminal A breast cancer is *HER2*$^-$, *ENG* could be affected by HER2 status in these cancer types. In our analysis, expression data was only obtained for Luminal A breast cancers not *HER2*$^+$ so differences in expression between the two were not analyzed.

Consistent with *TGFBR3*'s role as a tumor suppressor in many cancers, we found it to be a significant positive predictor of survival in all but two cancers (i.e., endometrial and all gastric subtypes, Fig. 2). Increased *TGFBR3* was predictive of response in all treatments and cancers we examined (Fig.4), further bolstering *TGFBR3*'s role as a negative regulator of tumor progression. Specifically, Bhola et al. (2013)[148] showed increased levels of *TGFBR3* in response to taxane in a small cohort (n = 17) of breast cancer patients; however, response to therapy was not analyzed. *TGFBR3* has been shown to act as a tumor suppressor in renal clear cell carcinoma[126] and non-small cell lung cancers[102] which was also confirmed here (Fig. 2). We were also able to expand *TGFBR3*'s role in renal cancer to papillary carcinomas as well (Fig. 2).

Expression of *ENG* and *TGFBR3* was not significantly different between wild-type and p53 mutated cancers indicating p53 likely does not impact expression itself. Whether protein secretion of these coreceptors is altered in these cancers is currently unknown, and cannot be ruled out, as previous studies have shown increased endoglin folding and maturation in p53 mutation settings. [149] TGFBR3 also undergoes N-linked glycosylation, so a similar scenario to endoglin is possible. Alterations in protein maturation could explain the differential patient outcomes observed between wild-type and p53 mutated cancers, when assessing for *ENG* and *TGFBR3*, despite changes in expression not being observed.

INHA's dependency on each coreceptor examined in survival analysis revealed distinct signatures between different cancer types (Table 1). Prior studies indicate a requirement for *ENG* in inhibin responsiveness and functions,[27] which was borne out in patient survival data here (Table 1). However, a few outliers exist such as p53 mutated breast and renal clear cell carcinoma where *INHA* was not always dependent on increased *ENG* and *TGFBR3* expression. We found *INHA* to only be a negative predictor of survival in patients expressing low *ENG* indicating *INHA* might act independent of either coreceptor in these cancer types. The role of other receptors involved in mediating *INHA*'s effects in these cancer types remains to be determined.

Gene signatures (Fig. 5) provided insights into how *INHA*, *TGFBR3,* or *ENG* would distinguish patients' outcomes. Some notable elements of this signature have been verified previously and even proposed as cancer biomarkers. For example, *EPHA2* overexpression has been associated with decreased patient survival and promotes drug resistance, increased invasion, and epithelial to mesenchymal transition (EMT).[150-153] HOXA1, a lncRNA overexpressed in cancers such as breast, melanoma, and oral carcinomas, drives metastasis and tamoxifen resistance.[154-156] For *TGFBR3* specifically, three genes revealed high discrimination between positive and negative outcomes: *UGT1A9* and *GLYATL1* were 25- and 35-fold more expressed in positive outcomes and *P2RX3* was 11.5-fold more expressed in negative outcomes. Of interest, UGT1A9 is a UDP-glucuronosyltransferase (UGT) whose activity has been implicated in drug resistance by affecting the bioactivity of the drug.[157,158] We speculate that as a proteoglycan, increased *TGFBR3* could compete for UDP-glucuronate acid (GlcA) and UDP-xylose, both key elements for UGT1A9 activity, thereby potentially disrupting UGT associated resistance mechanisms and increasing the efficacy of chemotherapy. We also narrowed down which pathways differentiated patient outcomes for either *INHA* or *TGFBR3*. For positive outcomes, we found that *INHA* was associated with PD-L1, Ras, and Rap1 signaling pathways. In adverse outcomes, *INHA* was associated with Hippo, Wnt, and cell cycle pathways. Wnt has been shown to regulate *INHA* transcription in rat adrenal cortex and could increase *INHA* expression in certain tumors to promote tumorigenesis.[159] Recent evidence indicates increased PD-L1 in dendritic cells in $INHA^{-/-}$ mice .[160] We speculate that increased *INHA* in tumors may inhibit PD-L1 expression perhaps via antagonistic effect on other TGF-β members, increasing anti-tumor immune responses.

There are currently no other cancer prognostic models based on our three assessed genes. The selected prognostic model showed high accuracy (96.7%) with 98.42% sensitivity and 91.56% specificity (Table 2). Moreover, most prognostic cancer models are directed to either a specific cancer type (e.g., breast, prostate) or a cancer stage (e.g., lymph node metastases, phases). Our model includes at least ten tumor types, is in the top two for sensitivity, and among the second quartile of specificities on assessment of 48 prognostic cancer models.[161-164] Thus, the *INHA-TGFBR3-ENG* signature has pan-cancer prognostic value.

Clustering analysis for genes correlated with *INHA*, *TGFBR3*, or *ENG* in cancers (Fig. 6) revealed *ENG* and *TGFBR3* had very few genes correlated exclusively to one or the other. As both receptors share similar structures and interact with common ligands,[38] this is not unexpected. Similarly, since *ENG* and *TGFBR3* had significant common gene associations this resulted in common pathways. For instance, a strong correlation with ECM-receptors and Rap1 signaling was observed. ENG has been shown to bind leukocyte integrins, promoting invasion,[165] and ECM remodeling during fibrosis.[166] TGFBR3 has been shown to regulate integrin localization and

adhesion to ECM.[167] *ENG* alone was associated with natural killer cell-mediated cytotoxicity consistent with previous findings showing anti-endoglin therapy augmented immune response in tumors by increasing NK cells, $CD4^{+,}$ and $CD8^{+}$ T lymphocytes.[168]

In conclusion, our pan-cancer analysis of the inhibin-activin network reveals a prognostic signature capable of accurately predicting patient outcome. Gene signatures from our analysis reveal robust relationships between *INHA*, *ENG*, and *TGFBR3* and other established cancer biomarkers. Survival analysis implicated members of the inhibin-activin network in cancers previously unstudied as well as corroborated previous findings. Further analysis of the role of the inhibin-activin network in cancer and relationship to other cancer associated genes, as well as validation as predictive biomarkers to chemotherapy is needed.

FUNDING

This work was supported by the National Institutes of Health (NIH) Grant 5R01CA21945 to Mythreye Karthikeyan (KM) and by the 2018-2.1.17-TET-KR-00001, 2018-1.3.1-VKE-2018-00032, and KH-129581 grants of the National Research, Development and Innovation Office, Hungary to BG.

CONFLICT OF INTEREST

None

REFERENCES

1 Schwartz, N. B. & Channing, C. P. Evidence for ovarian "inhibin": suppression of the secondary rise in serum follicle stimulating hormone levels in proestrous rats by injection of porcine follicular fluid. *Proc Natl Acad Sci U S A* **74**, 5721-5724, doi:10.1073/pnas.74.12.5721 (1977).

2 Keogh, E. J. *et al.* Selective suppression of FSH by testicular extracts. *Endocrinology* **98**, 997-1004, doi:10.1210/endo-98-4-997 (1976).

3 De Jong, F. H. & Sharpe, R. M. Evidence for inhibin-like activity in bovine follicular fluid. *Nature* **263**, 71-72, doi:10.1038/263071a0 (1976).

4 Setchell, B. P. & Jacks, F. Inhibin-like activity in rete testis fluid. *J Endocrinol* **62**, 675-676, doi:10.1677/joe.0.0620675 (1974).

5 Woodruff, T. K., Lyon, R. J., Hansen, S. E., Rice, G. C. & Mather, J. P. Inhibin and activin locally regulate rat ovarian folliculogenesis. *Endocrinology* **127**, 3196-3205, doi:10.1210/endo-127-6-3196 (1990).

6 Cate, R. L. *et al.* Isolation of the bovine and human genes for Müllerian inhibiting substance and expression of the human gene in animal cells. *Cell* **45**, 685-698, doi:10.1016/0092-8674(86)90783-x (1986).

7 Gaddy-Kurten, D. & Vale, W. W. Activin increases phosphorylation and decreases stability of the transcription factor Pit-1 in MtTW15 somatotrope cells. *J Biol Chem* **270**, 28733-28739, doi:10.1074/jbc.270.48.28733 (1995).

8 Makanji, Y. *et al.* Inhibin at 90: from discovery to clinical application, a historical review. *Endocr Rev* **35**, 747-794, doi:10.1210/er.2014-1003 (2014).

9 Ling, N. *et al.* A homodimer of the beta-subunits of inhibin A stimulates the secretion of pituitary follicle stimulating hormone. *Biochem Biophys Res Commun* **138**, 1129-1137, doi:10.1016/s0006-291x(86)80400-4 (1986).

10 Vale, W. *et al.* Purification and characterization of an FSH releasing protein from porcine ovarian follicular fluid. *Nature* **321**, 776-779, doi:10.1038/321776a0 (1986).

11 W., V., A., H., C., R. & J., Y. in *Peptide Growth Factors and Their Receptors II* Vol. 95 (Springer, Berlin, Heidelberg, 1990).

12 Antenos, M., Zhu, J., Jetly, N. M. & Woodruff, T. K. An activin/furin regulatory loop modulates the processing and secretion of inhibin alpha- and betaB-subunit dimers in pituitary gonadotrope cells. *J Biol Chem* **283**, 33059-33068, doi:10.1074/jbc.M804190200 (2008).

13 Robertson, D. M. *et al.* Isolation of inhibin from bovine follicular fluid. *Biochem Biophys Res Commun* **126**, 220-226, doi:10.1016/0006-291x(85)90594-7 (1985).

14 Rivier, J., Spiess, J., McClintock, R., Vaughan, J. & Vale, W. Purification and partial characterization of inhibin from porcine follicular fluid. *Biochem Biophys Res Commun* **133**, 120-127, doi:10.1016/0006-291x(85)91849-2 (1985).

15 Ueno, N. *et al.* Isolation and partial characterization of follistatin: a single-chain Mr 35,000 monomeric protein that inhibits the release of follicle-stimulating hormone. *Proc Natl Acad Sci U S A* **84**, 8282-8286, doi:10.1073/pnas.84.23.8282 (1987).

16 Miyamoto, K. *et al.* Isolation of porcine follicular fluid inhibin of 32K daltons. *Biochem Biophys Res Commun* **129**, 396-403, doi:10.1016/0006-291x(85)90164-0 (1985).

17 Attisano, L. & Wrana, J. L. Signal transduction by the TGF-beta superfamily. *Science* **296**, 1646-1647, doi:10.1126/science.1071809 (2002).

18 Attisano, L., Wrana, J. L., López-Casillas, F. & Massagué, J. TGF-beta receptors and actions. *Biochim Biophys Acta* **1222**, 71-80, doi:10.1016/0167-4889(94)90026-4 (1994).

19 Gray, P. C. *et al.* Identification of a binding site on the type II activin receptor for activin and inhibin. *J Biol Chem* **275**, 3206-3212, doi:10.1074/jbc.275.5.3206 (2000).

20 Attisano, L. *et al.* Identification of human activin and TGF beta type I receptors that form heteromeric kinase complexes with type II receptors. *Cell* **75**, 671-680, doi:10.1016/0092-8674(93)90488-c (1993).

21 Ebner, R., Chen, R. H., Lawler, S., Zioncheck, T. & Derynck, R. Determination of type I receptor specificity by the type II receptors for TGF-beta or activin. *Science* **262**, 900-902, doi:10.1126/science.8235612 (1993).

22 Attisano, L., Wrana, J. L., Montalvo, E. & Massagué, J. Activation of signalling by the activin receptor complex. *Mol Cell Biol* **16**, 1066-1073, doi:10.1128/mcb.16.3.1066 (1996).

23 Lewis, K. A. *et al.* Betaglycan binds inhibin and can mediate functional antagonism of activin signalling. *Nature* **404**, 411-414, doi:10.1038/35006129 (2000).

24 Zhu, J. *et al.* Inhibin α-subunit N terminus interacts with activin type IB receptor to disrupt activin signaling. *J Biol Chem* **287**, 8060-8070, doi:10.1074/jbc.M111.293381 (2012).

25 Chong, H. *et al.* Structure and expression of a membrane component of the inhibin receptor system. *Endocrinology* **141**, 2600-2607, doi:10.1210/endo.141.7.7540 (2000).

26 Chapman, S. C., Bernard, D. J., Jelen, J. & Woodruff, T. K. Properties of inhibin binding to betaglycan, InhBP/p120 and the activin type II receptors. *Mol Cell Endocrinol* **196**, 79-93, doi:10.1016/s0303-7207(02)00227-7 (2002).

27 Singh, P. *et al.* Inhibin Is a Novel Paracrine Factor for Tumor Angiogenesis and Metastasis. *Cancer Res* **78**, 2978-2989, doi:10.1158/0008-5472.CAN-17-2316 (2018).

28 López-Casillas, F. *et al.* Structure and expression of the membrane proteoglycan betaglycan, a component of the TGF-beta receptor system. *Cell* **67**, 785-795, doi:10.1016/0092-8674(91)90073-8 (1991).

29 Wang, X. F. *et al.* Expression cloning and characterization of the TGF-beta type III receptor. *Cell* **67**, 797-805, doi:10.1016/0092-8674(91)90074-9 (1991).

30 Gougos, A. & Letarte, M. Primary structure of endoglin, an RGD-containing glycoprotein of human endothelial cells. *J Biol Chem* **265**, 8361-8364 (1990).

31 Chen, W. *et al.* Beta-arrestin 2 mediates endocytosis of type III TGF-beta receptor and down-regulation of its signaling. *Science* **301**, 1394-1397, doi:10.1126/science.1083195 (2003).

32 McLean, S., Bhattacharya, M. & Di Guglielmo, G. M. βarrestin2 interacts with TβRII to regulate Smad-dependent and Smad-independent signal transduction. *Cell Signal* **25**, 319-331, doi:10.1016/j.cellsig.2012.10.001 (2013).

33 Blobe, G. C., Liu, X., Fang, S. J., How, T. & Lodish, H. F. A novel mechanism for regulating transforming growth factor beta (TGF-beta) signaling. Functional modulation of type III TGF-beta receptor expression through interaction with the PDZ domain protein, GIPC. *J Biol Chem* **276**, 39608-39617, doi:10.1074/jbc.M106831200 (2001).

34 Mythreye, K. & Blobe, G. C. The type III TGF-beta receptor regulates epithelial and cancer cell migration through beta-arrestin2-mediated activation of Cdc42. *Proc Natl Acad Sci U S A* **106**, 8221-8226, doi:10.1073/pnas.0812879106 (2009).

35 Lee, N. Y., Ray, B., How, T. & Blobe, G. C. Endoglin promotes transforming growth factor beta-mediated Smad 1/5/8 signaling and inhibits endothelial cell migration through its association with GIPC. *J Biol Chem* **283**, 32527-32533, doi:10.1074/jbc.M803059200 (2008).

36 Lee, N. Y. & Blobe, G. C. The interaction of endoglin with beta-arrestin2 regulates transforming growth factor-beta-mediated ERK activation and migration in endothelial cells. *J Biol Chem* **282**, 21507-21517, doi:10.1074/jbc.M700176200 (2007).

37 Cheifetz, S. *et al.* Endoglin is a component of the transforming growth factor-beta receptor system in human endothelial cells. *J Biol Chem* **267**, 19027-19030 (1992).

38 Kim, S. K., Henen, M. A. & Hinck, A. P. Structural biology of betaglycan and endoglin, membrane-bound co-receptors of the TGF-beta family. *Exp Biol Med (Maywood)* **244**, 1547-1558, doi:10.1177/1535370219881160 (2019).

39 Letamendía, A. *et al.* Role of endoglin in cellular responses to transforming growth factor-beta. A comparative study with betaglycan. *J Biol Chem* **273**, 33011-33019, doi:10.1074/jbc.273.49.33011 (1998).

599 40 Stenvers, K. L. *et al.* Heart and liver defects and reduced transforming growth factor
600 beta2 sensitivity in transforming growth factor beta type III receptor-deficient embryos.
601 *Mol Cell Biol* **23**, 4371-4385, doi:10.1128/mcb.23.12.4371-4385.2003 (2003).

602 41 Compton, L. A., Potash, D. A., Brown, C. B. & Barnett, J. V. Coronary vessel
603 development is dependent on the type III transforming growth factor beta receptor. *Circ*
604 *Res* **101**, 784-791, doi:10.1161/CIRCRESAHA.107.152082 (2007).

605 42 Li, D. Y. *et al.* Defective angiogenesis in mice lacking endoglin. *Science* **284**, 1534-1537,
606 doi:10.1126/science.284.5419.1534 (1999).

607 43 Arthur, H. M. *et al.* Endoglin, an ancillary TGFbeta receptor, is required for
608 extraembryonic angiogenesis and plays a key role in heart development. *Dev Biol* **217**,
609 42-53, doi:10.1006/dbio.1999.9534 (2000).

610 44 López-Novoa, J. M. & Bernabeu, C. The physiological role of endoglin in the
611 cardiovascular system. *Am J Physiol Heart Circ Physiol* **299**, H959-974,
612 doi:10.1152/ajpheart.01251.2009 (2010).

613 45 Miller, D. W. *et al.* Elevated expression of endoglin, a component of the TGF-beta-
614 receptor complex, correlates with proliferation of tumor endothelial cells. *Int J Cancer*
615 **81**, 568-572, doi:10.1002/(sici)1097-0215(19990517)81:4<568::aid-ijc11>3.0.co;2-x
616 (1999).

617 46 Jenkins, L. M., Horst, B., Lancaster, C. L. & Mythreye, K. Dually modified
618 transmembrane proteoglycans in development and disease. *Cytokine Growth Factor Rev*
619 **39**, 124-136, doi:10.1016/j.cytogfr.2017.12.003 (2018).

620 47 Mythreye, K. & Blobe, G. C. Proteoglycan signaling co-receptors: roles in cell adhesion,
621 migration and invasion. *Cell Signal* **21**, 1548-1558, doi:10.1016/j.cellsig.2009.05.001
622 (2009).

623 48 Gatza, C. E. *et al.* Type III TGF-β receptor enhances colon cancer cell migration and
624 anchorage-independent growth. *Neoplasia* **13**, 758-770, doi:10.1593/neo.11528 (2011).

625 49 Burrows, F. J. *et al.* Up-regulation of endoglin on vascular endothelial cells in human
626 solid tumors: implications for diagnosis and therapy. *Clin Cancer Res* **1**, 1623-1634
627 (1995).

628 50 Paauwe, M. *et al.* Endoglin targeting inhibits tumor angiogenesis and metastatic spread in
629 breast cancer. *Oncogene* **35**, 4069-4079, doi:10.1038/onc.2015.509 (2016).

630 51 Oxmann, D. *et al.* Endoglin expression in metastatic breast cancer cells enhances their
631 invasive phenotype. *Oncogene* **27**, 3567-3575, doi:10.1038/sj.onc.1211025 (2008).

632 52 Paauwe, M. *et al.* Endoglin Expression on Cancer-Associated Fibroblasts Regulates
633 Invasion and Stimulates Colorectal Cancer Metastasis. *Clin Cancer Res* **24**, 6331-6344,
634 doi:10.1158/1078-0432.CCR-18-0329 (2018).

635 53 Hempel, N. *et al.* Loss of betaglycan expression in ovarian cancer: role in motility and
636 invasion. *Cancer Res* **67**, 5231-5238, doi:10.1158/0008-5472.CAN-07-0035 (2007).

637 54 Gordon, K. J., Dong, M., Chislock, E. M., Fields, T. A. & Blobe, G. C. Loss of type III
638 transforming growth factor beta receptor expression increases motility and invasiveness
639 associated with epithelial to mesenchymal transition during pancreatic cancer
640 progression. *Carcinogenesis* **29**, 252-262, doi:10.1093/carcin/bgm249 (2008).

641 55 Turley, R. S. *et al.* The type III transforming growth factor-beta receptor as a novel tumor
642 suppressor gene in prostate cancer. *Cancer Res* **67**, 1090-1098, doi:10.1158/0008-
643 5472.CAN-06-3117 (2007).

644 56 Cook, L. M. *et al.* Betaglycan drives the mesenchymal stromal cell osteogenic program
645 and prostate cancer-induced osteogenesis. *Oncogene* **38**, 6959-6969, doi:10.1038/s41388-
646 019-0913-4 (2019).

647 57 Jovanović, B. *et al.* Transforming growth factor beta receptor type III is a tumor promoter
648 in mesenchymal-stem like triple negative breast cancer. *Breast Cancer Res* **16**, R69,
649 doi:10.1186/bcr3684 (2014).

650 58 Woszczyk, D. *et al.* Expression of TGF beta1 genes and their receptor types I, II, and III
651 in low- and high-grade malignancy non-Hodgkin's lymphomas. *Med Sci Monit* **10**, CR33-
652 37 (2004).

653 59 Zhang, J., Zhang, L., Lin, Q., Ren, W. & Xu, G. Prognostic value of endoglin-assessed
654 microvessel density in cancer patients: a systematic review and meta-analysis.
655 *Oncotarget* **9**, 7660-7671, doi:10.18632/oncotarget.23546 (2018).

656 60 Bai, S. *et al.* CD105 Is Expressed in Ovarian Cancer Precursor Lesions and Is Required
657 for Metastasis to the Ovary. *Cancers (Basel)* **11**, doi:10.3390/cancers11111710 (2019).

658 61 Zhang, J., Yuan, B., Zhang, H. & Li, H. Human epithelial ovarian cancer cells expressing
659 CD105, CD44 and CD106 surface markers exhibit increased invasive capacity and drug
660 resistance. *Oncol Lett* **17**, 5351-5360, doi:10.3892/ol.2019.10221 (2019).

661 62 Matzuk, M. M., Finegold, M. J., Su, J. G., Hsueh, A. J. & Bradley, A. Alpha-inhibin is a
662 tumour-suppressor gene with gonadal specificity in mice. *Nature* **360**, 313-319,
663 doi:10.1038/360313a0 (1992).

664 63 Shanbhag, S. A., Sheth, A. R., Nanivadekar, S. A. & Sheth, N. A. Immunoreactive
665 inhibin-like material in serum and gastric juice of patients with benign and malignant
666 diseases of the stomach. *Br J Cancer* **51**, 877-882, doi:10.1038/bjc.1985.133 (1985).

667 64 Suzuki, Y., Sugiyama, M., Abe, N., Fujioka, Y. & Atomi, Y. Immunohistochemical
668 similarities between pancreatic mucinous cystic tumor and ovarian mucinous cystic
669 tumor. *Pancreas* **36**, e40-46, doi:10.1097/mpa.0b013e3181584643 (2008).

65 McCluggage, W. G., Maxwell, P., Patterson, A. & Sloan, J. M. Immunohistochemical staining of hepatocellular carcinoma with monoclonal antibody against inhibin. *Histopathology* **30**, 518-522 (1997).

66 Arora, D. S. *et al.* Immunohistochemical expression of inhibin/activin subunits in epithelial and granulosa cell tumours of the ovary. *J Pathol* **181**, 413-418, doi:10.1002/(SICI)1096-9896(199704)181:4<413::AID-PATH789>3.0.CO;2-U (1997).

67 Huang, J. J. & Blobe, G. C. Dichotomous roles of TGF-β in human cancer. *Biochem Soc Trans* **44**, 1441-1454, doi:10.1042/BST20160065 (2016).

68 Ball, E. M., Mellor, S. L. & Risbridger, G. P. Cancer progression: is inhibin alpha from Venus or Mars? *Cytokine Growth Factor Rev* **15**, 291-296, doi:10.1016/j.cytogfr.2004.04.004 (2004).

69 Risbridger, G. P., Ball, E. M., Wang, H., Mellor, S. L. & Peehl, D. M. Re-evaluation of inhibin alpha subunit as a tumour suppressor in prostate cancer. *Mol Cell Endocrinol* **225**, 73-76, doi:10.1016/j.mce.2004.02.015 (2004).

70 Robertson, D. M., Pruysers, E. & Jobling, T. Inhibin as a diagnostic marker for ovarian cancer. *Cancer Lett* **249**, 14-17, doi:10.1016/j.canlet.2006.12.017 (2007).

71 Walentowicz, P. *et al.* Serum inhibin A and inhibin B levels in epithelial ovarian cancer patients. *PLoS One* **9**, e90575, doi:10.1371/journal.pone.0090575 (2014).

72 Balanathan, P. *et al.* Elevated level of inhibin-alpha subunit is pro-tumourigenic and pro-metastatic and associated with extracapsular spread in advanced prostate cancer. *Br J Cancer* **100**, 1784-1793, doi:10.1038/sj.bjc.6605089 (2009).

73 Mom, C. H. *et al.* Granulosa cell tumors of the ovary: the clinical value of serum inhibin A and B levels in a large single center cohort. *Gynecol Oncol* **105**, 365-372, doi:10.1016/j.ygyno.2006.12.034 (2007).

74 (https://ClinicalTrials.gov/show/NCT02429843).

75 (https://ClinicalTrials.gov/show/NCT01306058).

76 (https://ClinicalTrials.gov/show/NCT02560779).

77 (https://ClinicalTrials.gov/show/NCT01778530).

78 (https://ClinicalTrials.gov/show/NCT02664961).

79 (https://ClinicalTrials.gov/show/NCT01332721).

80 (https://ClinicalTrials.gov/show/NCT01328574).

81 (https://ClinicalTrials.gov/show/NCT01326481).

82 (https://ClinicalTrials.gov/show/NCT02520063).

83 (https://ClinicalTrials.gov/show/NCT03780010).

84 (https://ClinicalTrials.gov/show/NCT01375569).

85 (https://ClinicalTrials.gov/show/NCT01975519).

86 (https://ClinicalTrials.gov/show/NCT02396511).

87 (https://ClinicalTrials.gov/show/NCT02979899).

88 (https://ClinicalTrials.gov/show/NCT01806064).

89 (https://ClinicalTrials.gov/show/NCT00582985).

90 (https://ClinicalTrials.gov/show/NCT03418324).

91 (https://ClinicalTrials.gov/show/NCT03181308).

92 (https://ClinicalTrials.gov/show/NCT01727089).

93 (https://ClinicalTrials.gov/show/NCT01381861).

94 (https://ClinicalTrials.gov/show/NCT01090765).

95 (https://ClinicalTrials.gov/show/NCT02354612).

96 (https://ClinicalTrials.gov/show/NCT01564914).

97 (https://ClinicalTrials.gov/show/NCT01648348).

98 Schoonderwoerd, M. J. *et al.* Targeting endoglin expressing regulatory T cells in the tumor microenvironment enhances the effect of PD1 checkpoint inhibitor immunotherapy. *Clin Cancer Res*, doi:10.1158/1078-0432.CCR-19-2889 (2020).

99 Bandyopadhyay, A. *et al.* Systemic administration of a soluble betaglycan suppresses tumor growth, angiogenesis, and matrix metalloproteinase-9 expression in a human xenograft model of prostate cancer. *Prostate* **63**, 81-90, doi:10.1002/pros.20166 (2005).

100 Dong, M. *et al.* The type III TGF-beta receptor suppresses breast cancer progression. *J Clin Invest* **117**, 206-217, doi:10.1172/JCI29293 (2007).

101 Naumann, U. *et al.* Glioma gene therapy with soluble transforming growth factor-beta receptors II and III. *Int J Oncol* **33**, 759-765 (2008).

102 Finger, E. C. *et al.* TbetaRIII suppresses non-small cell lung cancer invasiveness and tumorigenicity. *Carcinogenesis* **29**, 528-535, doi:10.1093/carcin/bgm289 (2008).

103 Bandyopadhyay, A. *et al.* Antitumor activity of a recombinant soluble betaglycan in human breast cancer xenograft. *Cancer Res* **62**, 4690-4695 (2002).

104 Lee, J. D., Hempel, N., Lee, N. Y. & Blobe, G. C. The type III TGF-beta receptor suppresses breast cancer progression through GIPC-mediated inhibition of TGF-beta signaling. *Carcinogenesis* **31**, 175-183, doi:10.1093/carcin/bgp271 (2010).

105 Gallo-Oller, G. *et al.* P144, a Transforming Growth Factor beta inhibitor peptide, generates antitumoral effects and modifies SMAD7 and SKI levels in human glioblastoma cell lines. *Cancer Lett* **381**, 67-75, doi:10.1016/j.canlet.2016.07.029 (2016).

106 Llopiz, D. *et al.* Peptide inhibitors of transforming growth factor-beta enhance the efficacy of antitumor immunotherapy. *Int J Cancer* **125**, 2614-2623, doi:10.1002/ijc.24656 (2009).

107 Gao, J. *et al.* Integrative analysis of complex cancer genomics and clinical profiles using the cBioPortal. *Sci Signal* **6**, pl1, doi:10.1126/scisignal.2004088 (2013).

108 Cerami, E. *et al.* The cBio cancer genomics portal: an open platform for exploring multidimensional cancer genomics data. *Cancer Discov* **2**, 401-404, doi:10.1158/2159-8290.CD-12-0095 (2012).

109 Nagy, Á., Lánczky, A., Menyhárt, O. & Győrffy, B. Validation of miRNA prognostic power in hepatocellular carcinoma using expression data of independent datasets. *Sci Rep* **8**, 9227, doi:10.1038/s41598-018-27521-y (2018).

110 Fekete, J. T. & Gyorffy, B. ROCplot.org: Validating predictive biomarkers of chemotherapy/hormonal therapy/anti-HER2 therapy using transcriptomic data of 3,104 breast cancer patients. *Int J Cancer* **145**, 3140-3151, doi:10.1002/ijc.32369 (2019).

111 Oughtred, R. *et al.* The BioGRID interaction database: 2019 update. *Nucleic Acids Res* **47**, D529-D541, doi:10.1093/nar/gky1079 (2019).

112 Huang da, W., Sherman, B. T. & Lempicki, R. A. Systematic and integrative analysis of large gene lists using DAVID bioinformatics resources. *Nat Protoc* **4**, 44-57, doi:10.1038/nprot.2008.211 (2009).

113 Broad, D. *DepMap 20Q1 Public*. (2020).

114 Katayama, Y. *et al.* Clinical Significance of. *In Vivo* **31**, 565-571, doi:10.21873/invivo.11095 (2017).

115 Xiong, S., Klausen, C., Cheng, J. C., Zhu, H. & Leung, P. C. Activin B induces human endometrial cancer cell adhesion, migration and invasion by up-regulating integrin β3 via SMAD2/3 signaling. *Oncotarget* **6**, 31659-31673, doi:10.18632/oncotarget.5229 (2015).

763 116 Kita, A. *et al.* Activin B Regulates Adhesion, Invasiveness, and Migratory Activities in
764 Oral Cancer: a Potential Biomarker for Metastasis. *J Cancer* **8**, 2033-2041,
765 doi:10.7150/jca.18714 (2017).

766 117 Chen, Z. L., Qin, L., Peng, X. B., Hu, Y. & Liu, B. INHBA gene silencing inhibits gastric
767 cancer cell migration and invasion by impeding activation of the TGF-β signaling
768 pathway. *J Cell Physiol* **234**, 18065-18074, doi:10.1002/jcp.28439 (2019).

769 118 Li, Y. *et al.* Betaglycan (TGFBR3) Functions as an Inhibin A, but Not Inhibin B,
770 Coreceptor in Pituitary Gonadotrope Cells in Mice. *Endocrinology* **159**, 4077-4091,
771 doi:10.1210/en.2018-00770 (2018).

772 119 Makanji, Y., Harrison, C. A., Stanton, P. G., Krishna, R. & Robertson, D. M. Inhibin A
773 and B in vitro bioactivities are modified by their degree of glycosylation and their
774 affinities to betaglycan. *Endocrinology* **148**, 2309-2316, doi:10.1210/en.2006-1612
775 (2007).

776 120 Makanji, Y. *et al.* Suppression of inhibin A biological activity by alterations in the
777 binding site for betaglycan. *J Biol Chem* **283**, 16743-16751,
778 doi:10.1074/jbc.M801045200 (2008).

779 121 Wiater, E. *et al.* Endogenous betaglycan is essential for high-potency inhibin antagonism
780 in gonadotropes. *Mol Endocrinol* **23**, 1033-1042, doi:10.1210/me.2009-0021 (2009).

781 122 Meyers, R. M. *et al.* Computational correction of copy number effect improves
782 specificity of CRISPR-Cas9 essentiality screens in cancer cells. *Nat Genet* **49**, 1779-
783 1784, doi:10.1038/ng.3984 (2017).

784 123 Dempster, J. M. *et al.* Extracting Biological Insights from the Project Achilles Genome-
785 Scale CRISPR Screens in Cancer Cell Lines. *bioRxiv*, 720243, doi:10.1101/720243
786 (2019).

787 124 Ghandi, M. *et al.* Next-generation characterization of the Cancer Cell Line Encyclopedia.
788 *Nature* **569**, 503-508, doi:10.1038/s41586-019-1186-3 (2019).

789 125 Tsherniak, A. *et al.* Defining a Cancer Dependency Map. *Cell* **170**, 564-576.e516,
790 doi:10.1016/j.cell.2017.06.010 (2017).

791 126 Nishida, J., Miyazono, K. & Ehata, S. Decreased TGFBR3/betaglycan expression
792 enhances the metastatic abilities of renal cell carcinoma cells through TGF-β-dependent
793 and -independent mechanisms. *Oncogene* **37**, 2197-2212, doi:10.1038/s41388-017-0084-
794 0 (2018).

795 127 Frias, A. E., Li, H., Keeney, G. L., Podratz, K. C. & Woodruff, T. K. Preoperative serum
796 level of inhibin A is an independent prognostic factor for the survival of postmenopausal
797 women with epithelial ovarian carcinoma. *Cancer* **85**, 465-471, doi:10.1002/(sici)1097-
798 0142(19990115)85:2<465::aid-cncr26>3.0.co;2-w (1999).

128 Bashir, M., Damineni, S., Mukherjee, G. & Kondaiah, P. Activin-A signaling promotes epithelial-mesenchymal transition, invasion, and metastatic growth of breast cancer. *NPJ Breast Cancer* **1**, 15007, doi:10.1038/npjbcancer.2015.7 (2015).

129 Okano, M. *et al.* Significance of INHBA expression in human colorectal cancer. *Oncol Rep* **30**, 2903-2908, doi:10.3892/or.2013.2761 (2013).

130 Abrahao-Machado, L. F. & Scapulatempo-Neto, C. HER2 testing in gastric cancer: An update. *World J Gastroenterol* **22**, 4619-4625, doi:10.3748/wjg.v22.i19.4619 (2016).

131 Kim, S. K. *et al.* Structural Adaptation in Its Orphan Domain Engenders Betaglycan with an Alternate Mode of Growth Factor Binding Relative to Endoglin. *Structure* **27**, 1427-1442.e1424, doi:10.1016/j.str.2019.06.010 (2019).

132 Chang, H. Y. *et al.* Robustness, scalability, and integration of a wound-response gene expression signature in predicting breast cancer survival. *Proc Natl Acad Sci U S A* **102**, 3738-3743, doi:10.1073/pnas.0409462102 (2005).

133 Haider, S. *et al.* A multi-gene signature predicts outcome in patients with pancreatic ductal adenocarcinoma. *Genome Med* **6**, 105, doi:10.1186/s13073-014-0105-3 (2014).

134 Hallett, R. M., Dvorkin-Gheva, A., Bane, A. & Hassell, J. A. A gene signature for predicting outcome in patients with basal-like breast cancer. *Sci Rep* **2**, 227, doi:10.1038/srep00227 (2012).

135 Kim, S. Y. & Kim, Y. S. A gene sets approach for identifying prognostic gene signatures for outcome prediction. *BMC Genomics* **9**, 177, doi:10.1186/1471-2164-9-177 (2008).

136 Kanehisa, M. & Goto, S. KEGG: kyoto encyclopedia of genes and genomes. *Nucleic Acids Res* **28**, 27-30, doi:10.1093/nar/28.1.27 (2000).

137 Massagué, J. TGFbeta in Cancer. *Cell* **134**, 215-230, doi:10.1016/j.cell.2008.07.001 (2008).

138 Baldewijns, M. M. *et al.* High-grade clear cell renal cell carcinoma has a higher angiogenic activity than low-grade renal cell carcinoma based on histomorphological quantification and qRT-PCR mRNA expression profile. *Br J Cancer* **96**, 1888-1895, doi:10.1038/sj.bjc.6603796 (2007).

139 Das, S. & Marsden, P. A. Angiogenesis in glioblastoma. *N Engl J Med* **369**, 1561-1563, doi:10.1056/NEJMcibr1309402 (2013).

140 Longui, C. A. *et al.* Inhibin alpha-subunit (INHA) gene and locus changes in paediatric adrenocortical tumours from TP53 R337H mutation heterozygote carriers. *J Med Genet* **41**, 354-359, doi:10.1136/jmg.2004.018978 (2004).

141 Tremblay, J. J. & Viger, R. S. GATA factors differentially activate multiple gonadal promoters through conserved GATA regulatory elements. *Endocrinology* **142**, 977-986, doi:10.1210/endo.142.3.7995 (2001).

142 Gong, Y. *et al.* GATA4 inhibits cell differentiation and proliferation in pancreatic cancer. *PLoS One* **13**, e0202449, doi:10.1371/journal.pone.0202449 (2018).

143 Han, Q. *et al.* GATA4 is highly expressed in childhood acute lymphoblastic leukemia, promotes cell proliferation and inhibits apoptosis by activating BCL2 and MDM2. *Mol Med Rep* **16**, 6290-6298, doi:10.3892/mmr.2017.7369 (2017).

144 Nikiteas, N. I. *et al.* Vascular endothelial growth factor and endoglin (CD-105) in gastric cancer. *Gastric Cancer* **10**, 12-17, doi:10.1007/s10120-006-0401-8 (2007).

145 Chen, C.-Y. & Sheu, M.-J. Endoglin targeting inhibits tumor angiogenesis in non-small cell lung cancer. *The FASEB Journal* **32**, 695.616-695.616, doi:10.1096/fasebj.2018.32.1_supplement.695.16 (2018).

146 Henry, L. A. *et al.* Endoglin expression in breast tumor cells suppresses invasion and metastasis and correlates with improved clinical outcome. *Oncogene* **30**, 1046-1058, doi:10.1038/onc.2010.488 (2011).

147 Kauer, J. *et al.* CD105 (Endoglin) as negative prognostic factor in AML. *Sci Rep* **9**, 18337, doi:10.1038/s41598-019-54767-x (2019).

148 Bhola, N. E. *et al.* TGF-β inhibition enhances chemotherapy action against triple-negative breast cancer. *J Clin Invest* **123**, 1348-1358, doi:10.1172/JCI65416 (2013).

149 Vogiatzi, F. *et al.* Mutant p53 promotes tumor progression and metastasis by the endoplasmic reticulum UDPase ENTPD5. *Proc Natl Acad Sci U S A* **113**, E8433-E8442, doi:10.1073/pnas.1612711114 (2016).

150 Moyano-Galceran, L. *et al.* Adaptive RSK-EphA2-GPRC5A signaling switch triggers chemotherapy resistance in ovarian cancer. *EMBO Mol Med* **12**, e11177, doi:10.15252/emmm.201911177 (2020).

151 De Robertis, M. *et al.* Dysregulation of EGFR Pathway in EphA2 Cell Subpopulation Significantly Associates with Poor Prognosis in Colorectal Cancer. *Clin Cancer Res* **23**, 159-170, doi:10.1158/1078-0432.CCR-16-0709 (2017).

152 Zhuang, G. *et al.* Elevation of receptor tyrosine kinase EphA2 mediates resistance to trastuzumab therapy. *Cancer Res* **70**, 299-308, doi:10.1158/0008-5472.CAN-09-1845 (2010).

153 Huang, J. *et al.* EphA2 promotes epithelial-mesenchymal transition through the Wnt/β-catenin pathway in gastric cancer cells. *Oncogene* **33**, 2737-2747, doi:10.1038/onc.2013.238 (2014).

154 Kim, C. Y., Oh, J. H., Lee, J. Y. & Kim, M. H. The LncRNA HOTAIRM1 Promotes Tamoxifen Resistance by Mediating HOXA1 Expression in ER+ Breast Cancer Cells. *J Cancer* **11**, 3416-3423, doi:10.7150/jca.38728 (2020).

155 Bitu, C. C. *et al.* HOXA1 is overexpressed in oral squamous cell carcinomas and its expression is correlated with poor prognosis. *BMC Cancer* **12**, 146, doi:10.1186/1471-2407-12-146 (2012).

156 Wardwell-Ozgo, J. *et al.* HOXA1 drives melanoma tumor growth and metastasis and elicits an invasion gene expression signature that prognosticates clinical outcome. *Oncogene* **33**, 1017-1026, doi:10.1038/onc.2013.30 (2014).

157 Zimmer, B. M. *et al.* Loss of exogenous androgen dependence by prostate tumor cells is associated with elevated glucuronidation potential. *Horm Cancer* **7**, 260-271, doi:10.1007/s12672-016-0268-z (2016).

158 Allain, E. P., Rouleau, M., Lévesque, E. & Guillemette, C. Emerging roles for UDP-glucuronosyltransferases in drug resistance and cancer progression. *Br J Cancer* **122**, 1277-1287, doi:10.1038/s41416-019-0722-0 (2020).

159 Gummow, B. M., Winnay, J. N. & Hammer, G. D. Convergence of Wnt signaling and steroidogenic factor-1 (SF-1) on transcription of the rat inhibin alpha gene. *J Biol Chem* **278**, 26572-26579, doi:10.1074/jbc.M212677200 (2003).

160 de la Fuente-Granada, M., Olguín-Alor, R., Ortega-Francisco, S., Bonifaz, L. C. & Soldevila, G. Inhibins regulate peripheral regulatory T cell induction through modulation of dendritic cell function. *FEBS Open Bio* **9**, 137-147, doi:10.1002/2211-5463.12555 (2019).

161 Li, J. *et al.* A 5-Gene Signature Is Closely Related to Tumor Immune Microenvironment and Predicts the Prognosis of Patients with Non-Small Cell Lung Cancer. *Biomed Res Int* **2020**, 2147397, doi:10.1155/2020/2147397 (2020).

162 Ruiz, E. M. L. *et al.* A novel gene panel for prediction of lymph-node metastasis and recurrence in patients with thyroid cancer. *Surgery* **167**, 73-79, doi:10.1016/j.surg.2019.06.058 (2020).

163 Yang, H. *et al.* From big data to diagnosis and prognosis: gene expression signatures in liver hepatocellular carcinoma. *PeerJ* **5**, e3089, doi:10.7717/peerj.3089 (2017).

164 Huang, L. *et al.* Identification of a 7-gene signature that predicts relapse and survival for early stage patients with cervical carcinoma. *Med Oncol* **29**, 2911-2918, doi:10.1007/s12032-012-0166-3 (2012).

165 Torsney, E., Charlton, R., Parums, D., Collis, M. & Arthur, H. M. Inducible expression of human endoglin during inflammation and wound healing in vivo. *Inflamm Res* **51**, 464-470, doi:10.1007/pl00012413 (2002).

166 Alzahrani, A. *et al.* Endoglin haploinsufficiency is associated with differential regulation of extracellular matrix production during skin fibrosis and cartilage repair in mice. *J Cell Commun Signal* **12**, 379-388, doi:10.1007/s12079-018-0461-7 (2018).

167 Mythreye, K., Knelson, E. H., Gatza, C. E., Gatza, M. L. & Blobe, G. C. TβRIII/β-arrestin2 regulates integrin α5β1 trafficking, function, and localization in epithelial cells. *Oncogene* **32**, 1416-1427, doi:10.1038/onc.2012.157 (2013).

168 Jarosz, M. *et al.* Therapeutic antitumor potential of endoglin-based DNA vaccine combined with immunomodulatory agents. *Gene Ther* **20**, 262-273, doi:10.1038/gt.2012.28 (2013).

FIGURES

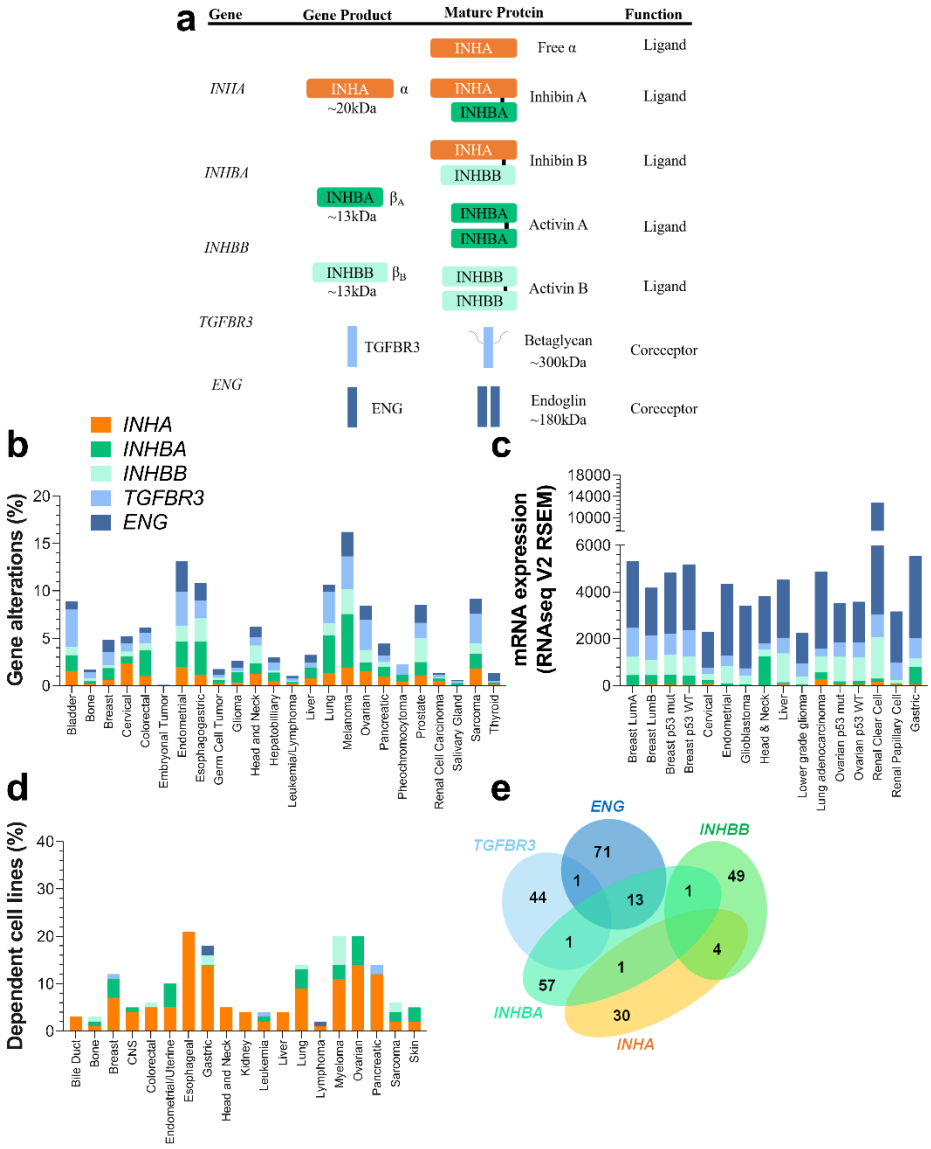

Figure 1. Expression and gene alterations of inhibin and activins. (a) Genes encoding INHA, INHBA, and INHBA produce monomeric α and β subunits. These subunits combine to form either homo or heterodimers representing mature inhibin A, inhibin B, activin A, and activin B. (b) TCGA base analysis of gene alteration frequencies of *INHA*, *INHBA*, *INHBB*, *TGBFR3,* and *ENG*. (c) Analysis of gene expression levels, also from TCGA sets, of the same genes as in (b) in a subset of cancer types and subtypes. Analysis included 16 studies and 6258 samples. (d) DepMap analysis of cell line dependency from indicated cancer types on each of the genes in (b). (e) Venn diagram illustrating the number of common dependent genes for each gene in (b). All numeric data are available in Supplementary Table 1. Abbreviations – CNS: Central Nervous System; LumA: Luminal A; LumB: Luminal B; mut: mutated; WT: wild-type.

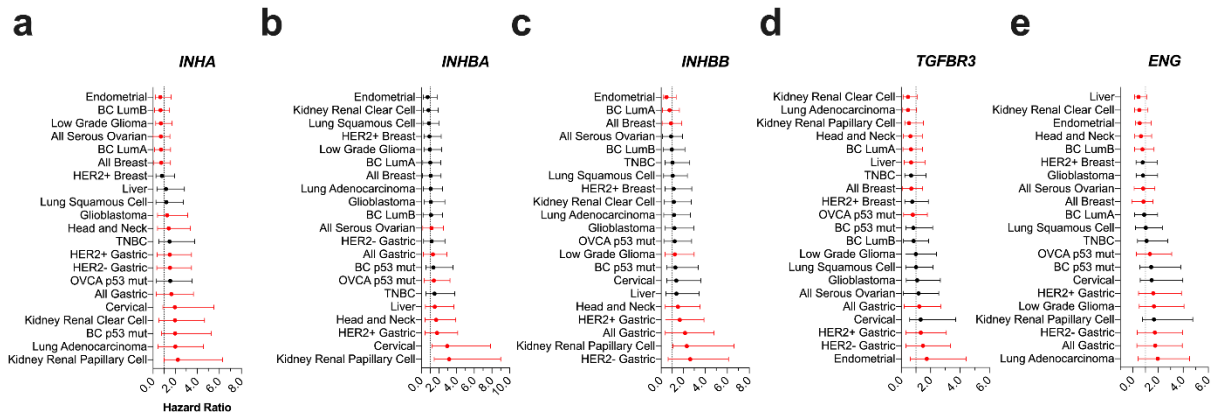

Figure 2. Impact of *INHA, INHBA, INHBB, TGFBR3, and ENG* on patient survival in indicated cancers. (a) Forest Plot with Hazard Ratios (HR) of indicated genes generated from KM Plotter or data from cBioportal. Black dots represent HR that are not statistically significant ($p > 0.05$) and red dots represent HR that are statistically significant ($p < 0.05$). All numeric data are available in Supplementary Table 2.

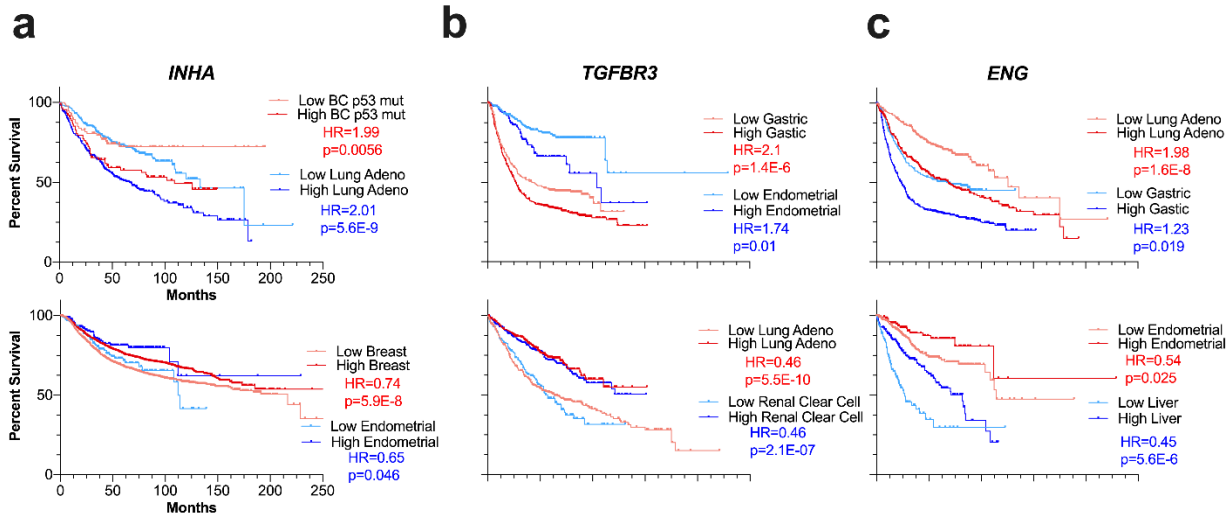

Figure 3. Representative Kaplan Meier curves for *INHA*, *TGFBR3*, and *ENG*. Event-free survival in indicated cancers using median to separate expression (lighter shade indicates bottom patients expressing bottom 50% and darker shade top 50%). Survival curves represent OS for all cancers except breast cancer (RFS) and ovarian cancer (PFS). Top plots show cancer types where the gene is a negative predictor of survival, and bottom plots show cancer types where the gene is a negative predictor.

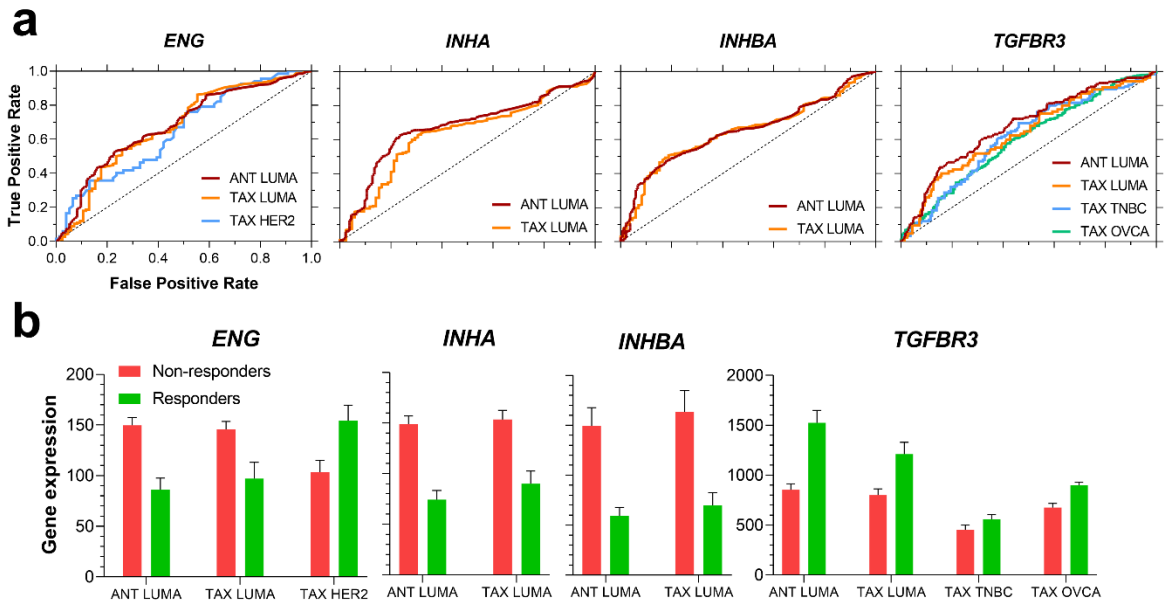

939
940 **Figure 4. ROC plots (a) and gene expression (b) of indicated genes for different**
941 **chemotherapy regimens.** (a) ROC curves, in which performance ability was verified (i.e., AUC >
942 0.6), were plotted for *ENG*, *INHA*, *INHBA,* and *TGFBR3*. (b) Gene expression for each
943 investigated gene between responders and non-responders for the assessed pharmacological
944 treatments. Abbreviations: ANT: anthracycline; TAX: taxane; LUMA: luminal A; TNBC: triple-
945 negative breast cancer; OVCA: serous ovarian cancer.

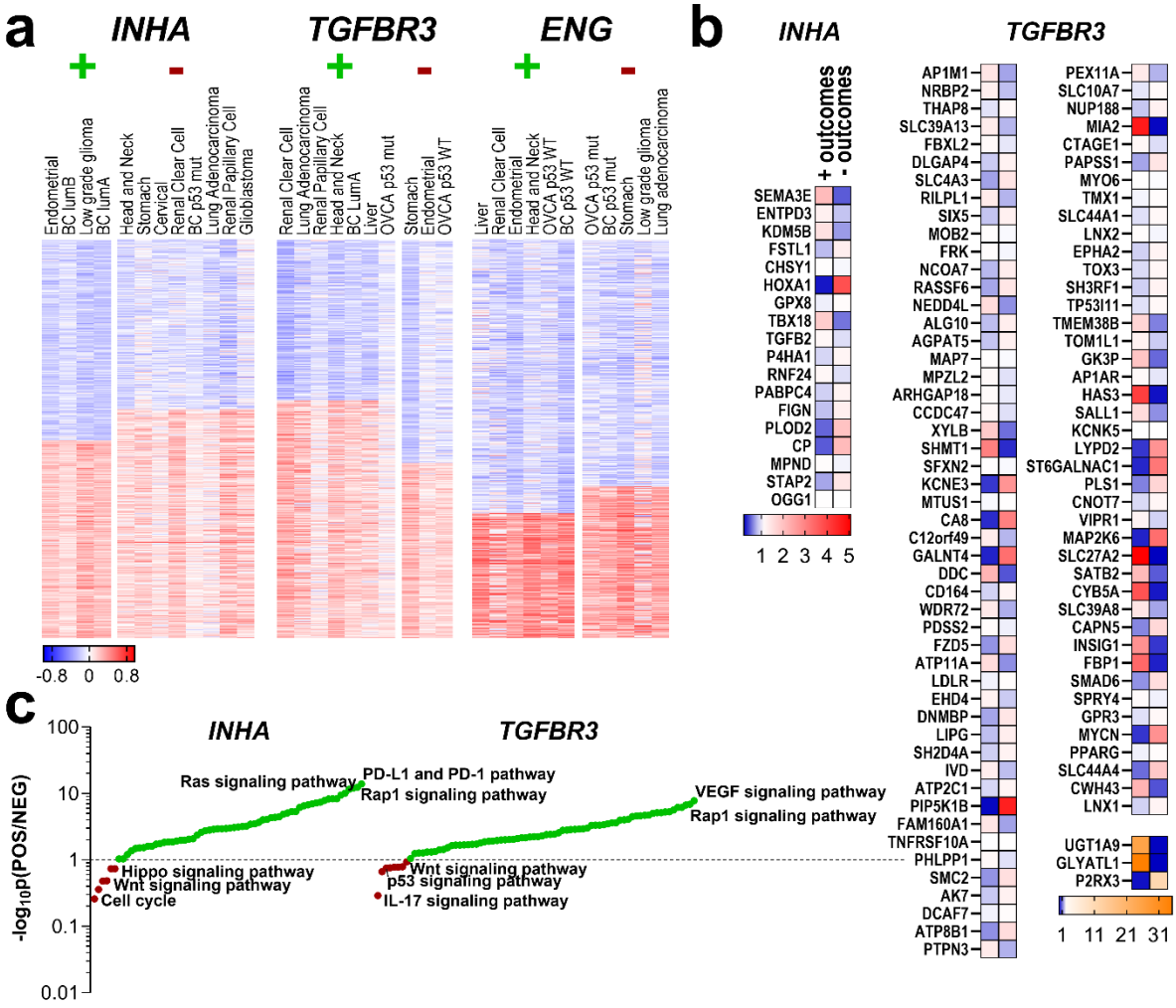

Figure 5. Gene signatures and expression patterns for cancers where *INHA*, *TGFBR3,* or *ENG* predicted survival outcomes. (a) Cancer types in which either *INHA TGFBR3* or *ENG* had either positive (+) or negative (-) survival outcomes had their RNA-seq gene data correlation clustered for either low or high degree of correlations to each *INHA, TGFBR3* or *ENG* as indicated. (b) mRNA abundance of a subset of common genes obtained from pairwise comparisons of the top correlated genes from the positive outcome with the genes that had lower correlations in the negative outcome set, and vice-versa. mRNA expression was assessed in each cancer set.* $p < 0.05$ ** $p < 0.01$ *** $p < 0.001$ **** $p < 0.0001$ (c) Pathway analysis after BioGRID assessment of the significant genes from (b), ranked with a ratio of significance between sets from the positive and negative outcomes for each gene.

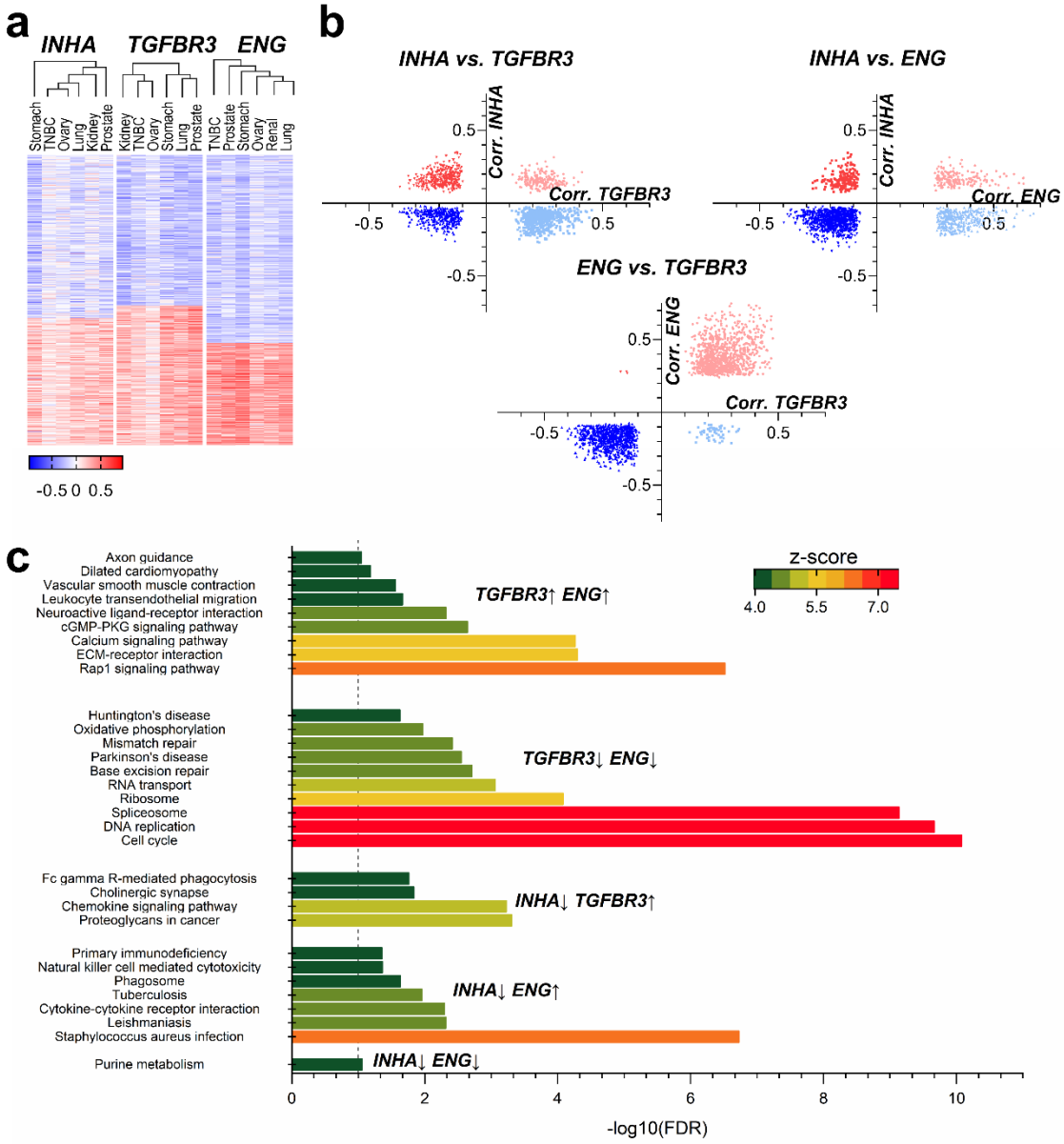

Figure 6. Functional analysis of gene signatures between *INHA* and *TGFBR3* and *INHA* and *ENG*. (a) Supervised clustering of correlations of RNA-seq data between *INHA*, *TGFBR3,* and *ENG* was performed to obtain sets of positive and negatively correlated genes for each set. (b) Common genes that were found in each group of correlated genes (e.g., negative correlation to *INHA vs.* positive to *TGFBR3* and all combinations) is presented. (c) KEGG pathway analysis for groups of genes correlated with the indicated combination. Unique pathways with an FDR below 0.05 were identified for the comparisons and are presented.

TABLES

Table 1. p values and Hazard Ratios (HR) from survival curves assessing the relationship between *TGFBR3/ENG* and *INHA* on patient survival. Survival curves were generated in KM Plotter for all cancer types. Survival curves represent overall survival, progression free survival (marked with *), or relapse free survival (marked with #) for patients expressing high or low mRNA (split by median) of the indicated gene.

Type	Subtype	Variable	*INHA*	*TGFBR3*	*INHA and TGFBR3*	*INHA in High TGFBR3 Patients*	*INHA in Low TGFBR3 Patients*
Breast#	All	p value	5.9E-8	4E-11	4.5E-12	.00026	5.9E-6
		Hazard Ratio (HR)	.74	.69	.68	.74	.74
	p53 Mutated	p value	.0056	.41	.82	.27	.015
		Hazard Ratio (HR)	1.99	.82	.95	1.5	2.29
Ovarian*	All	p value	1.5E-6	.047	.16	.096	.0032
		Hazard Ratio (HR)	.71	1.16	.9	1.18	.82
	p53 Mutated	p value	.00039	.039	.1	.021	.00075
		Hazard Ratio (HR)	1.55	.79	.83	1.51	1.74
Lung	All	p value	.00029	3.4E-7	1.4E-6	4.4E-5	.18
		Hazard Ratio (HR)	1.26	.65	.73	1.49	1.12
	Adenocarcinoma	p value	5.6E-9	5.5E-10	3.1E-7	1.7E-5	1.6E-8
		Hazard Ratio (HR)	2.01	.46	.53	2.49	1.98
Kidney	Renal Clear Cell	p value	7.1E-06	2.1E-7	3.3E-05	.2	9.0E-06
		Hazard Ratio (HR)	1.98	.46	.53	1.42	2.75

Type	Subtype	Variable	*INHA*	*ENG*	*INHA and ENG*	*INHA in High ENG Patients*	*INHA in Low ENG Patients*
Breast#	All	p value	5.9E-8	.0014	7.4E-6	.0043	.0027
		Hazard Ratio (HR)	.74	.84	.78	.79	.79
	p53 Mutated	p value	.0056	.12	.057	.26	.035
		Hazard Ratio (HR)	1.99	1.46	1.6	.69	2.24
Ovarian*	All	p value	1.5E-6	.0032	.00011	.00016	.065
		Hazard Ratio (HR)	.71	.82	.77	.71	.83
	p53 Mutated	p value	.00039	.0098	.00091	1.8E-6	.18
		Hazard Ratio (HR)	1.55	1.36	1.49	2.12	.8
Lung	All	p value	.00029	.0056	.063	.47	5.8E-8
		Hazard Ratio (HR)	1.26	1.2	1.13	1.07	1.66
	Adenocarcinoma	p value	5.6E-9	1.6E-8	5.6E-12	.14	.00041
		Hazard Ratio (HR)	2.01	1.98	2.3	1.25	2.12
Kidney	Renal Clear Cell	p value	7.1E-06	8.6E-6	4.5E-05	.072	2.5E-06
		Hazard Ratio (HR)	1.98	.51	.53	1.53	2.6

Table 2. Prognostic performance of each delineated probit model. For either an *INHA or TGFBR3* model, the described cancer types and subtypes used to analyze the positive (+), and negative (-) outcomes are shown. The number of genes in each model, the model's specificity (i.e., how the model certifies true positives), sensitivity (i.e., how the model certifies true negatives), and their false positive and false negative ratios are shown. The correct classification ratio is also highlighted below.

	***INHA* model**	***TGFBR3* model**
Cancer types (+)	• Endometrial; • BC lum A; • BC lum B; • Low grade glioma	• Renal Clear Cell; • Lung adenocarcinoma; • Renal Papillary Cell; • Head and Neck; • BC lum A; • Liver; • OVCA p53 mut
Cancer types (-)	• Head and Neck; • Stomach; • Cervical; • Renal Clear Cell; • BC p53 mut; • Lung adenocarcinoma; • Renal Papillary Cell; • Glioblastoma.	• Stomach; • Endometrial; • OVCA p53 WT.
Genes in model	43	37
Specificity	90.76%	98.42%
Sensitivity	93.17%	91.56%
False positives ratio	6.83%	8.44%
False negative ratio	9.24%	1.58%
Accuracy	**92.25%**	**96.70%**